A Comparative Study on the Thermal Decomposition Behaviors between β-Cyclodextrin and Its Inclusion Complexes of Organic Amines

Le Xin Song* and Peng Xu

Department of Chemistry, University of Science and Technology of China, Hefei, 230026, Anhui, China

Received: July 08, 2008; Revised Manuscript Received: September 12, 2008

How does a complexed organic guest change its thermal stability during the heating process? How does the guest release influence the decomposition behavior of the complexed host? To answer these questions, in-situ Fourier transform infrared spectroscopy and gas chromatography coupled to time-of-flight mass spectrometry with programmed temperature were employed in the present work. The careful comparisons among the thermal decomposition behaviors of free β-cyclodextrin (β-CD) and its inclusion complexes of ethylenediamine and diethylenetriamine indicated that the release of the amines was not a simple physical process without the rupture of chemical bonds but was instead a complex process together with the fragments from complexed β-CD. In short, the release and decomposition of the complexed amines drove the decomposition of the complexed β-CD in their respective inclusion complexes. It was found that the thermal decomposition behavior of the complexed β-CD was influenced by the complexed amines dependent on the nature of the amines, and at the same time, β-CD had, to a certain extent, changed the temperature of the phase-change, release, and decomposition of organic amines by the formation of inclusion complexes with them.

Introduction

β-Cyclodextrin (β-CD, Figure 1) is a cyclic α-1,4-linked glucose oligomer containing seven α-D-glucose units. Owing to its geometry, it easily forms inclusion complexes with a variety of guest molecules.[1−3] Many of the inclusion complexes have been advantageously utilized in food, pharmaceutical, and cosmetic products.[4−6] Ethylenediamine and diethylenetriamine (EDA and DTA, Figure 1) are both typical amino-functional organic compounds and have been widely applied to different chemical problems and, in particular, to the study of synthetic organic chemistry, coordination chemistry, and supramolecular chemistry.[7−9]

To examine or control the temperature of phase-change, release, and decomposition of the guest is one of the prospective studies concerning solid inclusion complexes in supramolecular chemistry.[10,11] However, very few papers have concentrated on how a guest is released and what the effect of the guest release is on thermal decomposition behavior of survived host during follow-up. It is currently one of the most important and intriguing problems in cyclodextrin chemistry not only because it has practical significance of β-CD inclusion complexes for medicine, food additive, cosmetics ingredient, biological products, and the like but also because it has implications for the way in which we should view the differences in the intermolecular interactions among free, complexed, and survived β-CD (see Figure 1).

In practice, the decomposition processes of inclusion complexes of β-CD are mostly investigated by means of thermogravimetry (TG) analysis,[12,13] which only provides information about mass change. To the best of our knowledge, the below problems have not been investigated systematically so far. For example, when and how is the complexed guest set free? How does the release of the complexed guest partly or completely influence the thermal decomposition of the complexed or survived β-CD? What are the decomposition modes of free, complexed, and survived β-CD? EDA and DTA as multiamine compounds are constitutively active because of an unshared electron pair at amino nitrogen atoms. It was found that they can form the inclusion complexes with β-CD because of intermolecular interaction between the host and the guest.[14] The differences in both TG profiles and decomposition kinetics results of the two inclusion complexes also have been observed in a recent paper.[14] Additionally, the comparison between the TG curves of β-CD and its complexes of the two guests indicates that the intermolecular complexation between EDA and β-CD effectively improves the thermal stability of EDA. Contrarily, the complexation between DTA and β-CD considerably reduces the thermal stability of DTA.[15] The phenomena can be attributed to different host−guest interaction intensities in the inclusion systems.[16−18] However, there is no explicit description of how such interactions could lead to an effect on the decomposition of the complexed β-CD, especially the survived β-CD. In the present work, we try to examine the relationship between

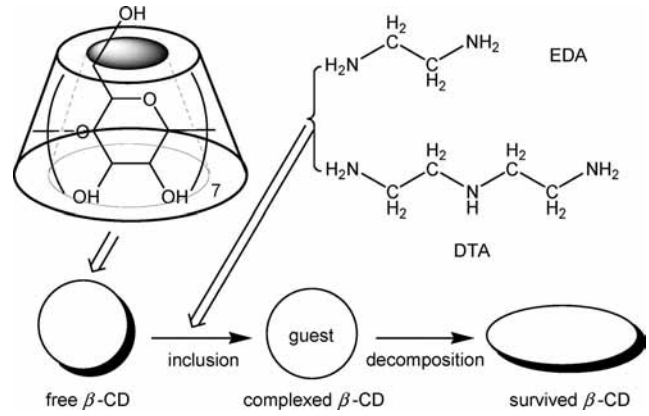

Figure 1. A schematical drawing illustrating the formation and decomposition of the inclusion complexes of β-CD with EDA and DTA.

* Author to whom correspondence should be addressed. E-mail: solexin@ustc.edu.cn.

10.1021/jp806026q CCC: $40.75
Published on Web 10/18/2008

TABLE 1: Appointed Heating Program for the Samples

step	temperature range (/K)	heating rate (/K·min^{-1})	retained time (/min)
1	303	0	3
2	303−363	80	5
3	363−463	80	6
4	463−553	80	7
5	553−653	80	5
6	653−773	100	3

intermolecular interactions and thermal decomposition behaviors of free, complexed, and survived β-CD. As such, we believe that it will make a major contribution to the research and application of β-CD inclusion complexes.

Electrospray ionization mass spectrometry (ESI-MS) was employed to characterize noncovalent interactions. Both in-situ Fourier transform infrared (FTIR) spectroscopy and gas chromatography coupled to time-of-flight mass spectrometry (GC-TOF-MS) with programmed temperature were carried out to investigate the thermal decomposition behaviors of free β-CD and its inclusion complexes with the objective of trying to find details regarding the decomposition process of samples.

Experimental Section

Materials. β-CD was purchased from Shanghai Chemical Reagent Company and was recrystallized twice from deionized water. The organic amines, EDA and DTA, were purchased from Shanghai Chemical Reagent Company and were used without further purification. All other reagents were of analytical reagent grade unless stated otherwise.

Preparation of the Inclusion Complexes. The solid inclusion complexes were prepared and purified according to the reported method.[14] The host−guest stoichiometric ratios of the two solid inclusion complexes, EDA-β-CD and DTA-β-CD, were determined to be 2:5 and 1:1 on the basis of the results of elemental analysis and the analysis of ^{1}H NMR data.[15] The host−guest stoichiometries of the two complexes in aqueous solution were both determined to be 1:1 by means of UV−vis spectrophotometry by use of 1-naphthol as a probe.[19] The difference in chemical stoichiometry for the complex of EDA with β-CD in solid state and in aqueous solution reveals the complexity and multiformity of the intermolecular complexation process taking place between them.

Instruments and Methods. ESI-MS was carried out on an LTQ linear ion-trap mass spectrometer produced by ThermoFisher Scientific. Samples were injected via a syringe pump at a rate of 1−3 μL/min. Nebulizer gas was nitrogen and ion spray voltage was 5 kV. Data for each sample were acquired for 2 min in the mass range of m/z 150−2000.

In-situ FTIR spectra were recorded on a Bruker EQUINOX55 spectrometer in the range 4000−400 cm^{-1}. High-temperature cell (HTC-3) and automatic temperature controller (ATC-24−1) were made by Harrick Scientific Products, Inc. Data for each sample were obtained every 10 K with a heating rate of 5 K·min^{-1} in the air.

GC-TOF-MS was carried out with a Micromass GCT-MS spectrometer using the standard direct insertion probe for solid samples with an increasing temperature. Experimental conditions are summarized in Table 1.

Three types of diagrams are collected: (1) the variation of total ion current (TIC) in intensity as a function of heating time, (2) the variation of ion current for a selected individual fragment in intensity as a function of heating time, and (3) mass spectra at specific time points on the basis of the appointed heating program. Computer analysis allows extraction of signals with temporal structure.

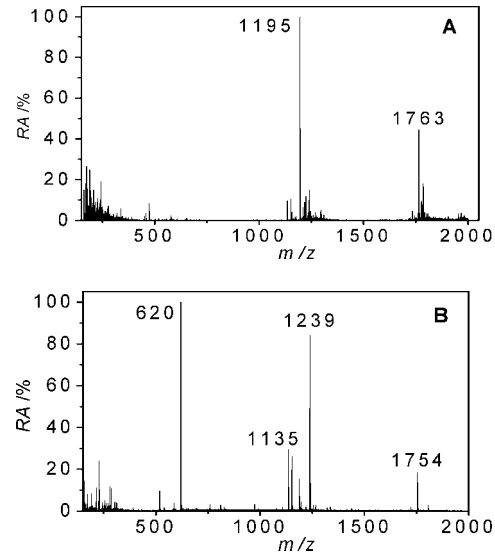

Figure 2. ESI mass spectra of EDA-β-CD (A) and DTA-β-CD (B).

Results and Discussion

A Direct Proof of the Formation of Two Inclusion Complexes, EDA-β-CD and DTA-β-CD, under the Conditions of ESI-MS. As a soft ionization technique, ESI-MS has been playing an important role in describing the host−guest noncovalent complexation of β-CD with an organic guest because of many advantages over other techniques, such as high sensitivity, rapid speed, and low sample consumption.[20−22]

The features of ESI-MS for EDA-β-CD and DTA-β-CD in the positive ion mode are illustrated in Figure 2A and 2B, respectively. Several significant molecule−ion peaks making establishment of molecular formulas of the two inclusion complexes straightforward are clearly observed on the basis of the exact locations of these peaks and their relative abundance (*RA*).

The strongest signal at m/z 1195 is traced back to the [EDA-β-CD]$^+$ of EDA-β-CD. By comparison, the peak intensity of β-CD at m/z 1135 is rather weak (*RA* < 10%) in Figure 2A. In addition, a peak at m/z 1763 with an *RA* value of 44.37% is ascribed to the ion [2EDA-3β-CD]$^{2+}$. The result indicates the presence of the intermolecular interaction between EDA and β-CD even under the conditions of ESI-MS.

In Figure 2B, the molecule−ion peaks at m/z 620, 1135, 1239, and 1754 are attributed to [DTA-β-CD]$^{2+}$, [β-CD]$^+$, [DTA-β-CD]$^+$, and [DTA-3β-CD]$^{2+}$, respectively. The data also point out the formation of the inclusion complex, that is, DTA-β-CD under the conditions of ESI-MS.

It is obvious, therefore, that only 1:1 stoichiometry may be envisaged under the current conditions according to the ESI mass spectra of EDA-β-CD and DTA-β-CD. The stabilities of the two inclusion complexes of β-CD with the two organic amines are rather different. For example, their stability constants (K_s) in aqueous solution were estimated to be 83.4 and 368.0 mol^{-1}·dm^3 by UV−vis spectrophotometry by use of 1-naphthol as a probe.[19] Moreover, an experimental investigation on the thermal decomposition kinetics shows that the apparent activation energies (E_a) of β-CD, EDA-β-CD, and DTA-β-CD during thermal decomposition process were 86.2, 34.4, and 84.2 kJ·mol^{-1}, respectively, according to Ozawa theory.[14] Clearly, there is a considerable difference in the values of both K_s and

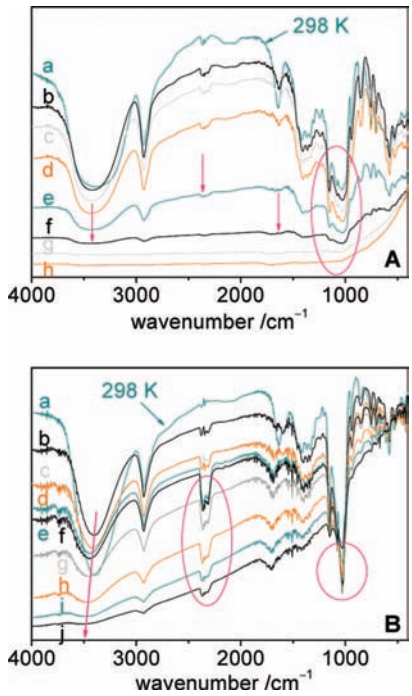

Figure 3. In-situ FTIR spectra of (A) free β-CD from 493 to 553K (b−h) and (B) DTA-β-CD from 493 to 573K (b−j) at intervals of 10 K.

E_a between the two complexes reflecting their different stabilities. These results were caused by the minor structural difference of the two guests.

A Difference in in-Situ FTIR Spectra between Free β-CD and DTA-β-CD. The thermal decomposition behaviors of free β-CD and DTA-β-CD are investigated by in-situ FTIR spectroscopy to evaluate whether there are significant differences in the main thermal decomposition mode between the free β-CD and the complexed β-CD in DTA-β-CD.

As may be seen from the FTIR curve of free β-CD at 298 K in Figure 3A, the absorption bands at 1157, 1080, and 1029 mainly correspond to the stretch vibrations of C−O and C−O−C of glucose units of β-CD, and the bands at 2923 and 3427 cm^{-1} are due to the symmetric stretching vibration of CH_2 groups and the stretching vibration of OH groups of β-CD, respectively. The band at 1640 cm^{-1} is ascribed to the OH bending vibration. The absorption around 2360 cm^{-1} is assigned as the antisymmetric stretching vibration of CO_2 molecules arising from CO_2 in an ambient air test environment.[23,24]

The differences in the decomposition profiles between free β-CD and DTA-β-CD are summarized as follows:

(1) There are different intensity changes in the absorption signal of CO_2 at 2360 cm^{-1} between the two samples with the increase of temperature. The intensities of the band from free β-CD decrease gradually from 298 to 523 K, and they almost disappear at 533 K and above. However, the band from the complexed β-CD is clearly observed even at 573 K. The intensity of the band becomes stronger and stronger from 298 to 533 K and then decreases slowly up to 573 K. The finding reflects that the mechanism of this decomposition reaction is more complicated than that of free β-CD.

(2) There are significant differences in intensity and shape of the vibration bands of C−O and C−O−C at 1157, 1080, and 1029 cm^{-1} between the two samples. The intensities of the bands in the free β-CD decrease gradually from 298 to 533 K, and they disappear above 543 K. The two phenomena correspond to partial and complete decomposition of the free β-CD, respectively. The bands look like a combination of a broad signal and its left shoulder. However, though the intensities of the bands in the complexed β-CD also decrease gradually from 298 to 573 K, they do not disappear even at a higher temperature of 573 K. In addition, there is a sharp signal at 1029 cm^{-1} appearing in all the 10 curves. The phenomena indicate that the complexed β-CD is more stable than free β-CD.

(3) There are different intensity and position changes in the broad band of OH at 3427 cm^{-1} as well as in the narrow band of OH at 1640 cm^{-1} between the two samples. The intensities of the bands in the free β-CD decrease gradually from 298 to 533 K, and they almost disappear at 543 K and above. The decrease of absorption is caused by the loss of OH which comes from earlier water and later β-CD. At the same time, the absorption intensities at 945 and 857 cm^{-1} because of the stretch vibration of C−O of glucose units decrease synchronously. These observations imply that the rapid dissociation of β-CD begins at around 543 K. However, for the complexed β-CD, on one hand, the broad band shifts to a higher wavenumber and disappears at a higher temperature of 573 K. On the other hand, along with the losses of water and DTA, the OH bending vibration at 1640 cm^{-1} does not disappear even at 573 K suggesting that though the OH groups can still exist in the survived fragments of the DTA-β-CD, their vibration modes have been limited. The survived fragments of the complexed β-CD can be regarded as the survived β-CD.[25] Further, there are no obvious signals in curves g and h in free β-CD, but those signals due to β-CD even in curves i and j still exist in the sample of DTA-β-CD. Clearly, these phenomena can be explained as the effect of the complexed amines on the stack structure of β-CD molecules because the different molecular stack will lead to the different hydrogen interaction between β-CD molecules.

Synoptically speaking, the comparison of variations in infrared absorption signal strength between free β-CD and the complexed β-CD reflects that the latter has a higher heat-resistant ability than the former. That is to say, free β-CD has a limited heat-resistant ability, but the complexed as well as the survived β-CD has a higher heat-resistant ability. To achieve the deep and comprehensive understanding of the thermal decomposition differences between free β-CD and the complexed β-CD, GC-TOF-MS measurement is performed to investigate the detailed decomposition processes of the samples.

A Short Description about GC-TOF-MS Measurement System. Thermoanalytical techniques such as TG and DSC are frequently used to investigate the thermal properties of β-CD and its inclusion complexes, but they only display the change of mass or energy when a sample is continuously heated.[26,27] However, GC-TOF-MS measurement system equipped with a direct sample injection valve and temperature-programmed heating chamber can provide information on the chemical composition of the split fragments, which allows us to illustrate the decomposition approach of the sample.

Three kinds of graphs, that is, TIC graphs, thermal trace curves of fragments, and mass spectra on the thermal decomposition processes of the three samples, have been constructed in this work to investigate the thermal decomposition differences between free β-CD and complexed β-CD in its inclusion complexes with two organic amines.

A Direct Comparison in TIC Profiles among Free β-CD, EDA-β-CD, and DTA-β-CD. The plots of TIC versus heating time of free β-CD and its two inclusion complexes are shown in Figure 4. The curves a, b, and c are ascribed to free β-CD, EDA-β-CD, and DTA-β-CD, respectively. The decomposition

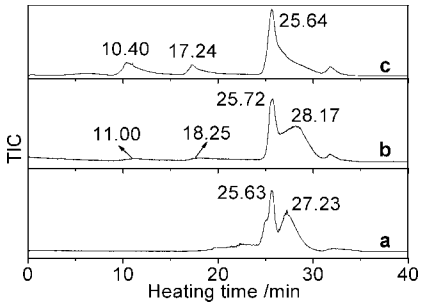

Figure 4. TIC curves of free β-CD (a), EDA-β-CD (b), and DTA-β-CD (c).

processes of the samples are controlled by the temperature program as described in the Experimental Section. A low-temperature gap can appear when the real temperature of a sample fails to catch up with the rapid rise of the surrounding temperature. The sample will continue to be heated and will decompose as the surrounding temperature is sustained at the required level for a while. Thus, the change of the TIC values mainly occurs at a relative stable level for the surrounding temperature.

The appointed temperature levels are selected according to the TG analyses of the samples. Their TG profiles are reported in a recent paper.[14] In the temperature range from 373 to 573 K, free β-CD does not lose any mass, but its two inclusion complexes decrease their mass all the way. For instance, the TG curve of DTA-β-CD shows three stages of mass loss. Thus, the appointed temperature levels are selected to be at 463 (stage one), 553 (stage two), and 653 K (stage three) corresponding to heating time ranges of 10.00−16.00, 17.12−24.12, and 25.37−30.37 min, respectively, in the heating program of the GC-TOF-MS system.

As can be seen from Figure 4, there are two obvious peaks at 10.40 and 17.24 min in curve c before the appearance of the main peak of DTA-β-CD at 25.64 min. Contrastively, the peaks of EDA-β-CD at 11.00 and 18.25 min are quite weak in curve b. Clearly, the peaks are attributed to the release of the organic amines from their respective inclusion complexes because, as would be expected, there are no such kinds of peaks of free β-CD in curve a.

Again, the TIC profiles indicate that the positions and shapes of the main peaks of the samples are different from one another. First, the main peak of free β-CD at 25.63 min appears earlier in comparison with those of its two inclusion complexes implying that it begins to decompose slightly earlier than its inclusion complexes. Second, the shapes and numbers of the main peaks in the TIC curves of the three samples are significantly different in the heating time range from 20 to 30 min. DTA-β-CD presents a single strong peak at 25.64 min (curve c), but the other two show similar double peaks, that is, a major peak and a minor right shoulder peak (curves a and b).

The important differences in the TIC profiles among the samples allow us to conclude that the existence and nature of organic amines must influence the thermal decomposition behavior of the complexed β-CD even if the amines are released from their respective inclusion complexes of β-CD. The magnitude of the influence depends, to some extent, on the nature of the amines. This can occur because the different amine molecules have, to a different extent, promoted the interaction between β-CD molecules during the formation of an inclusion complex. The observation is in good agreement with that from in-situ FTIR spectra.

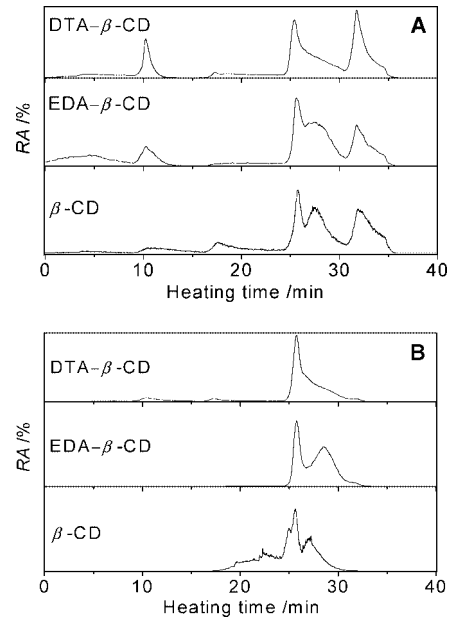

Figure 5. MID curves of key fragments: *m*/*z* at 43.99 (A) and *m*/*z* at 60.02 (B).

Thermal Trace Curves for Several Key Fragments. In multiple ion detection mode (MID), the ion currents belonging to the selected individual *m*/*z* species of the three samples are detected, and their values of *RA* are plotted against heating time in Figure 5.

Figure 5 displays the MID curves of two key fragments that appeared in all three samples. The fragment of *m*/*z* at 43.99 in Figure 5A is identified as CO_2^+, which is the decomposition product of glucopyranose units. At about 10 min, that is, at the third step of the applied heating program, the values of *RA* of CO_2^+ in the two inclusion complexes are obviously higher than that of it in free β-CD, and the *RA* value of CO_2^+ in DTA-β-CD is larger than that of it in EDA-β-CD, suggesting that the release of the amines drives the decomposition of the two kinds of complexed β-CD, each to a different extent. However, the release-driven decomposition only occurs slightly in the light of the TIC curves described before. Also, the peaks of CO_2^+ in the three samples are observed in a rather high and wide temperature range.

The fragment of *m*/*z* at 60.02 in Figure 5B also comes from the glucopyranose units.[25] In the time range from 20 to 30 min, that is, at the fourth and fifth steps of the heating program, the shapes of the three curves are rather different. The starting time of the fragment release in the two inclusion complexes is seriously delayed because of the intermolecular interactions between the host and the guest[16−18] as well as between hosts. The results agree with those from IR and TIC. Interestingly, upon release, the intensity of the fragment peak increases abruptly.

MS Analysis on the Thermal Decomposition Process of Free β-CD. First, the surrounding temperature is kept at 463 K in the time range from 10 to 16 min to eliminate the temperature difference between the inside of the test samples and their surroundings. It is seen from Figure 6A that free β-CD already has started to decompose. The disruption of chemical bonds only produces a few free radicals or other reactive species. Obviously, the fragments of *m*/*z* at 43.99 (*RA*, 100.0%), 57.03 (13.20%), and 60.02 (40.33%) are CO_2^+, $C_3H_5O^+$, and $C_2H_4O_2^+$, respectively. Actually, they are relative to the rupture initiation of the bonds of C−O and C−C in the glucopyranose as well as of the 1,4-glycosidic bonds.

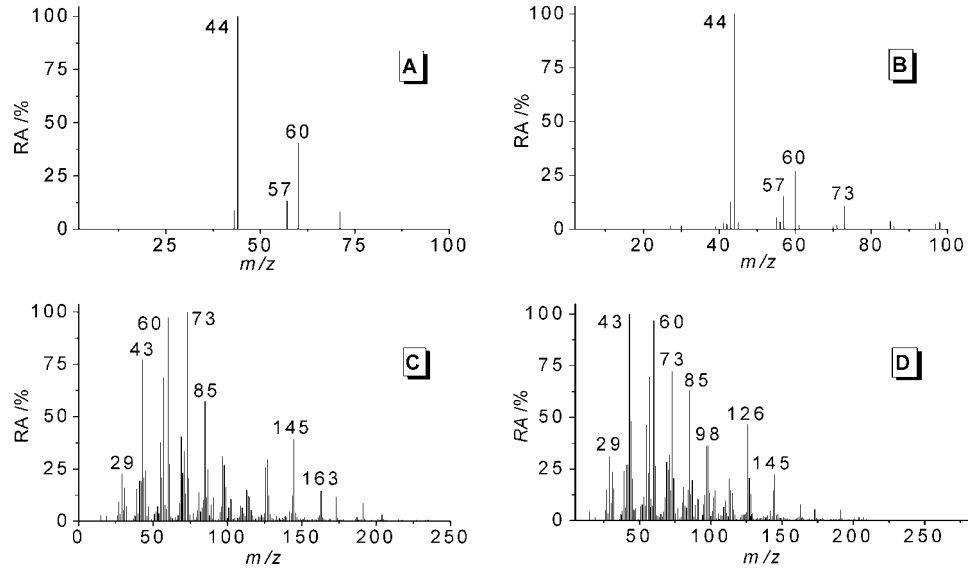

Figure 6. Mass spectra of free β-CD at 10.17 (A), 17.33 (B), 25.41 (C), and 26.33 min (D).

Second, when the environment is kept at 553 K from 17.12 to 24.12 min, more small fragments with low values of *RA* less than 6% are observed in Figure 6B. Otherwise, the positions and relative intensities of three major fragments are similar to those in Figure 6A even with an increment of temperature of 90 K. No peaks with *m/z* at higher than 100 appear in the two figures. For these reasons, it is possible to hypothesize that only a few glucopyranose units have been broken down to pieces; free β-CD has not decomposed to any important extent. This has been proved by the TIC graph of free β-CD in Figure 4.

Third, as the temperature rises from 553 to 653 K, the decomposition behavior of free β-CD escalates to a crisis (see Figure 4a). When compared with the two figures described above, Figure 6C shows a large number of additional fragments with higher values of *RA* and *m/z*. In other words, many new fragments are found in the figure, such as the fragments of *m/z* at 29.00 (*RA*, 22.67%), 85.03 (57.14%), and 163.06 (14.43%) are CHO^+, $C_4H_5O_2^+$, and $C_6H_{11}O_5^+$, respectively. Besides, the *RA* values of many fragments also are greatly enhanced, such as the fragments of *m/z* at 43.02 ($C_2H_3O^+$, 77.16%), 60.02 (97.62%), and 73.03 ($C_3H_5O_2^+$, 100.0%). Also, the peak at *m/z* 73.03 has become the strongest instead of that at *m/z* 43.99 in Figure 6A and 6B.

Fourth, when continuing to increase the temperature, the sample indicates the strongest peak with *m/z* at 43.02 in Figure 6D.

The results indicate that the thermal decomposition mode of free β-CD is dependent on heating temperature and time. We try to illustrate two rupture modes (I and II) of chemical bonds in the decomposition path of free β-CD to small fragments on the basis of the findings in this study (Figure 6A−D).

As can be seen in Figure 7, in mode I, the disruption of one glucose unit mainly produce three types of fragments of *m/z* at 43.99, 57.03, and 60.02. The mode is relatively simple corresponding to the thermal decomposition of lower temperature region.

In mode II, the rupture of 1,4-glycosidic bonds not only induces the formation of a new fragment CHO^+ but also results in the rupture of more bonds of C−C and C−O in glucose units. Also, mode II describes that there are several possibilities of the covalent bond ruptures in the glucopyranose of β-CD. It is reasonable that the larger fragments will be split into smaller ones under the increased temperature. However, according to

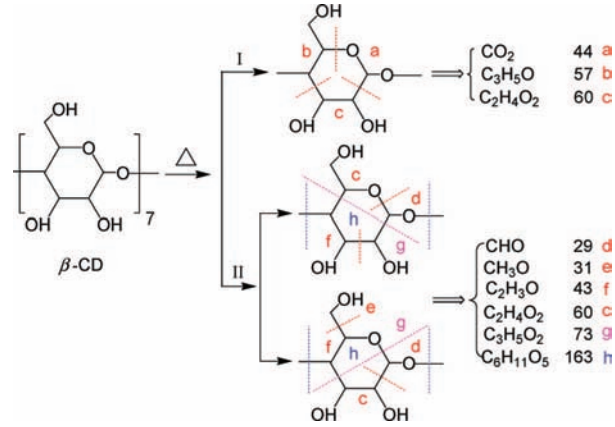

Figure 7. Proposed two rupture modes of chemical bonds in the decomposition path of free β-CD to small fragments in the lower (I) and higher (II) temperature regions.

Figure 6C and 6D, CO_2^+ is not one of the main dissociation products under high temperature.

To make a direct comparison in decomposition mode between free and complexed β-CD, several key problems need to be solved. For example, whether such decomposition of β-CD is influenced by a guest molecule? If yes, what is the influence? Where is the difference between the influences of two guests?

MS Analyses on the Decomposition Processes of EDA-β-CD and DTA-β-CD. Attention is paid to the detailed comparison among the thermal decomposition processes for free β-CD and its inclusion complexes in this section. EDA and DTA are short-chain alkyl di- and triamines, respectively. Clearly, the molecular sizes and chain lengths of the two amines are different from each other. It is well-known that β-CD has different binding abilities to different guests even if the guests possess very similar structure.[28] We now aim at evaluating the effect of the different intermolecular interactions between β-CD and similar guests on the thermal decomposition behaviors of a complexed β-CD in several different heating stages. A series of mass spectra of the two inclusion complexes are collected and given in Figures 8, 10, and 11.

When the surrounding temperature of the samples is kept at 463 K, that is, in the time range from 10 to 16 min (see Figure 8), it is clear to see that the existence of EDA, especially DTA

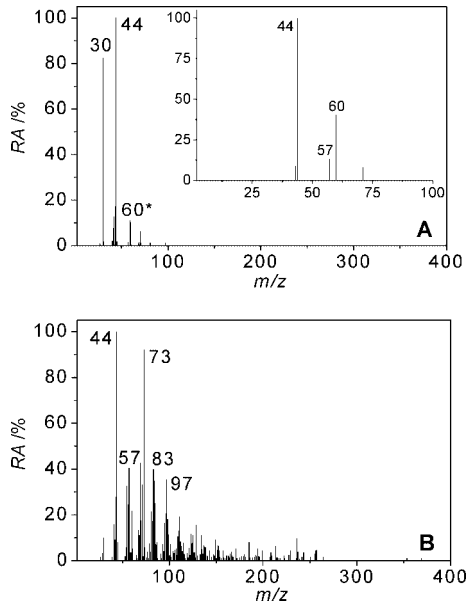

Figure 8. Mass spectra of EDA-β-CD (A) and DTA-β-CD (B) at 10.17 min. The inset of A is the mass spectrum of free β-CD at 10.17 min.

with a longer chain, complicates markedly thermal decomposition behavior.

As can be seen in Figure 8A, the fragments of *m/z* at 30.03 (CH_4N^+, 82.41%) and 60.07 (denoted by 60*, $C_2H_8N_2^+$, 10.09%) both come from the guest EDA. In comparison with the mass spectrum of free β-CD in 10.17 min, no fragments appearing in Figure 6A are observed in Figure 8A except for the fragment with *m/z* 43.99. The observations indicate that the stability of the complexed β-CD for EDA-β-CD seems to be higher than that of free β-CD at 463 K.

The fragments of DTA-β-CD at 10.17 min in Figure 8B are mainly because of the large decomposition of guest DTA, such as those of *m/z* at 44.05 ($C_2H_6N^+$, 61.57%) and at 73.08 ($C_3H_9N_2^+$, 92.02%). At the same time, all the fragments in Figure 6A, that is, the inset of Figure 8A, are present in Figure 8B, and the *RA* value of the strong peak with *m/z* at 43.99 because of CO_2^+ in Figure 6A, which comes from a glucose unit, does not change in the case of both EDA-β-CD and DTA-β-CD. It is interesting that not only the fragment amount of DTA-β-CD is much larger than that of EDA-β-CD but also many fragments in the mass spectrum of DTA-β-CD are found to contain H, N, and O atoms simultaneously. The results indicate that the complexed β-CD in EDA-β-CD has a higher thermal stability than that in DTA-β-CD at 463 K. It is well-known that a solid inclusion complex molecule consists of complexed hosts and complexed guests in a certain stoichiometry. The stability of the inclusion complex in solid state is dependent not only on the association ability between the complexed hosts and the complexed guests but also on their respective stabilities to heat including their phase characteristics such as phase-change temperature in their respective inclusion complexes (see Figure 9).

The boiling point of DTA (475.2 K) is obviously higher than that of EDA (390.7 K), and the surrounding temperature of the samples at 463 K is just between their boiling points. Therefore, we consider that the abnormal behavior of the thermal decomposition of DTA-β-CD as well as the marked differences in the thermal decomposition products between the two inclusion complexes may involve the relative strength among three kinds of intermolecular interactions, that is, host−host, host−guest, and guest−guest. The larger the difference of these forces, the larger will be the difference of the decomposition behaviors for the samples and the smaller will be their contribution to the stabilities of the samples. This can be caused by the variation of the chain length in the two amines. Theoretically, as can be seen in Figure 9, after liquefaction of the complexed guests, the van de Waals interaction among the EDA molecules should be weaker than that among the DTA molecules.

The kinds and amounts of the fragments, in which there are many oxygen atoms because of β-CD, corresponding to the release of DTA are more than those of the fragments corresponding to the release of EDA indicating that the interaction between the complexed β-CD molecules in DTA-β-CD is weaker than that between the complexed β-CD molecules in EDA-β-CD. Furthermore, DTA seems to be more easily released from its complex of β-CD than EDA on the basis of the comparison between the TIC curves b and c in Figure 4. The phenomena cannot be explained by the different interaction strengths between β-CD and the amines because our results from PM3 calculations according to a similar method described in a recent paper[26] indicate that the interaction energy (−65.0 kJ·mol^{-1} in vacuo and −71.8 kJ·mol^{-1} in water) between β-CD and DTA with a longer chain is markedly lower than the interaction energy (−40.7 kJ·mol^{-1} in vacuo and −45.0 kJ·mol^{-1} in water) between β-CD and EDA with a shorter chain both in vacuo and in water. This finding implies that the intermolecular interaction strengths between β-CD and the amines in solid state could be significantly different from those between β-CD and the amines in vacuo and in water.

The fragment information in Figure 10A and 10B is significantly more than that in Figure 6B, that is, the inset of Figure 10A. The release of EDA and DTA from the samples is still in progress at this time, that is, at 17.33 min.

In Figure 10A, many new fragment peaks appear when compared with Figure 8A. The decomposition of EDA is greatly affected by the decomposition of β-CD since there are many fragments that contain both N and O atoms, such as the fragments of *m/z* at 94.05 ($C_2H_8NO_3^+$, 15.34%), 122.08 ($C_2H_{10}N_4O_2^+$, 9.63%), and 163.10 ($C_5H_{14}N_3O_3^+$, 3.15%). This result is one of the important clues for the simultaneous decomposition of EDA and β-CD at this temperature. The strongest peak at *m/z* 43.99 (CO_2, 100%) in Figure 6B is not observed in Figure 10A, but a novel peak with *m/z* at 44.99 ($COOH^+$, 2.99%) is found. Nonetheless, the typical fragments due to the decomposition of β-CD, such as *m/z* at 57.03 ($C_3H_5O^+$) and 60.02 ($C_2H_4O_2^+$), possess only low *RA* values of 6.48% and 1.55%, respectively.

The fragments, such as *m/z* at 44.05 ($C_2H_6N^+$, 82.05%) and 73.08 ($C_3H_9N_2^+$, 100%), have very strong signals in Figure 10B. Their existence provides a direct proof for the further release and decomposition of DTA. Besides, the *RA* values of the two fragments of *m/z* at 43.99 (100.0%) and 60.02 (26.92%) in Figure 6B are severely weakened to 9.63% and 11.87%, respectively. By appearances, the amount of the fragments in Figure 10B seems to be reduced by the further release of DTA. However, we have to take into consideration the fact that many of them contain both N and O atoms. Therefore, it should be reasonable that the release process of DTA refers to the rupture and formation of chemical bonds.

The mass spectra involving the fragment information of EDA-β-CD and DTA-β-CD at 25.41 min are shown in Figure 11A and 11B, respectively. Although the profiles of the figures for the two inclusion complexes are somewhat similar to each other

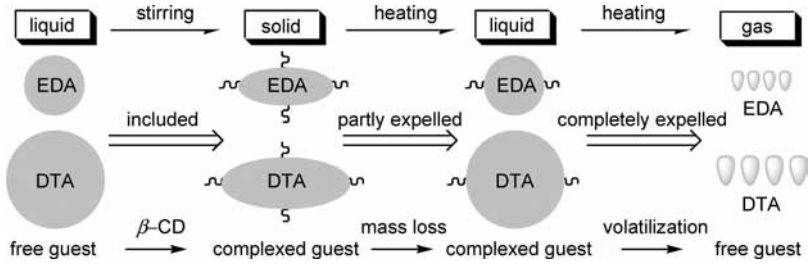

Figure 9. A schematic drawing depicting the phase changes of EDA and DTA before and after inclusion by β-CD.

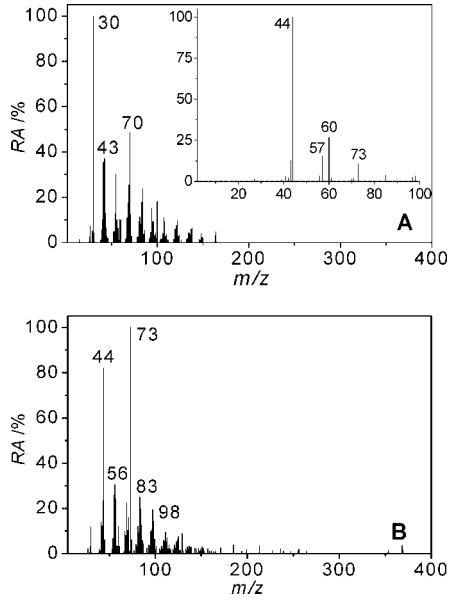

Figure 10. Mass spectra of EDA-β-CD (A) and DTA-β-CD (B) at 17.33 min. The inset of A is the mass spectrum of free β-CD at 17.33 min.

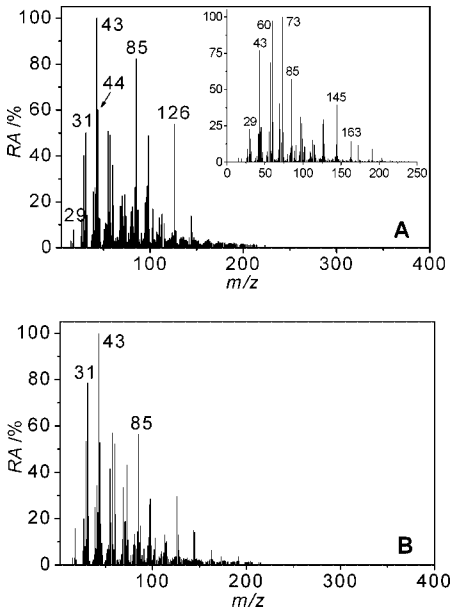

Figure 11. Mass spectra of EDA-β-CD (A) and DTA-β-CD (B) at 25.41 min. The inset of A is the mass spectrum of free β-CD at 25.41 min.

in appearance, they are greatly different from that of Figure 6C for free β-CD at 25.41 min.

At this time, the decomposition of free β-CD is progressed according to mode II in Figure 7. As described before, there are three main strong peaks in Figure 6C, that is, the inset of Figure 11A, corresponding to the fragments of *m*/*z* at 73.03 (100.0%), 60.02 (97.62%), and 43.02 (77.16%). However, at the same heating time, the *RA* values of the peaks are changed into 24.98, 34.66, and 100.0% for EDA-β-CD and into 43.18, 52.40, and 100.0% for DTA-β-CD. In other words, the order of the *RA* values of the fragment peaks is just reversed, and the first strongest peak corresponds to the small fragment with *m*/*z* at 43.02 ($C_2H_3O^+$). Additionally, the fragments of *m*/*z* at 31.02 and 85.03 both have large *RA* values of more than 49.50% in the samples of the two complexes. Interestingly, the *RA* value of the fragment peak at 43.99 because of CO_2^+ has also significantly increased from 19.2% in β-CD to more than 52.82% in the two complexes at the same temperature. The finding is in accordance with the result of IR observations in the antisymmetric stretching vibration of CO_2 at 2360 cm^{-1}. In IR spectrum of free β-CD, the small peak at 2360 cm^{-1} can be clearly seen at 513 K and below in the curves a−d of Figure 3A. However, when the sample is heated to a higher temperature such as 523 K and above, because the fragment of CO_2 is no longer one of the main decomposition products, the signal of the peak in IR spectra at first decreases (curves from d to f) and then disappears (curves g and h). However, when the sample of DTA-β-CD is heated, the fragment of CO_2 is detected both in a lower temperature region and in a higher temperature region (Figure 3B). CO_2 becomes one of the main decomposition products all the time. Thus, the absorption intensity of CO_2 presents an increasing trend (curves from a to g) in the IR spectrum. Subsequently, because of the sample loss, the intensity of the signal of CO_2 (curves from g to j) decreases slowly. It is important and instructive that, like the high-temperature region, no observable peaks attributing to the amines are found in Figure 11A and 11B.

The results strongly suggest that the decomposition mode of the β-CD molecules complexed by different amines has been fundamentally changed even if the amines originally included in the cavity of β-CD have been expelled from their inclusion complexes completely. The results of the decomposition kinetics experiments about the systems support the view that there are different decomposition activation energies among β-CD and its inclusion complexes of the amines.[14]

The proposed decomposition modes III and IV are illustrated in Figure 12. Only so-called survived β-CD molecules[23] are still left in samples after all of the amine molecules are fully expelled. There is an interaction between the amines and β-CD in light of our recent study.[14] The NH_2 groups at the end of EDA or DTA molecular chain can form hydrogen bonds with the OH groups on the rim of the β-CD cavity.

As depicted in Figure 9, when an inclusion complex is heated to a certain extent, the amines having low melting point and boiling point are changed into liquid from solid at first and then lose their masses because of volatilization and, finally, are rapidly released after reaching the boiling point. At a higher temperature, the disruption extent of the complexed and survived

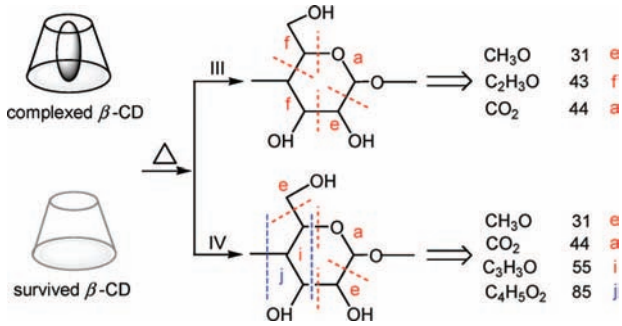

Figure 12. Proposed decomposition modes for the complexed and survived β-CD at high temperature.

β-CD molecules will be spread along those broken line boundaries. The 2-C, 3-C, and 6-C on the glucose units are connected with OH groups, and so the small fragments expressed in Figure 12 are easily formed around these sites. Such a process is greatly influenced by the nature of the lost amines because they can lead to a new stack frame of the complexed β-CD differently from that of free β-CD.

The order of the calculated values of E_a for β-CD, EDA-β-CD, and DTA-β-CD is β-CD (86.2 kJ$\cdot$mol^{-1}) > DTA-β-CD (84 kJ$\cdot$mol^{-1}) > EDA-β-CD (34.4 kJ$\cdot$mol^{-1}),[14] which is not in agreement with the result of the thermal stabilities of the samples β-CD < DTA-β-CD < EDA-β-CD on the basis of the measurements by GC-TOF-MS. The significant difference between them implies the complexity of the thermal decomposition processes of the samples. Additionally, the minor difference in temperature response between IR and GC-TOF-MS measurements can be caused by the difference on the current experimental circumstance (IR in air, GC-TOF-MS in vacuum) and different heating rates (IR, 5 K$\cdot$min^{-1}; GC-TOF-MS, 80 K$\cdot$min^{-1}).

Conclusion

In summary, for the inclusion complexes of β-CD with the amines, the release of complexed amine molecules drives the decomposition of complexed β-CD, and at the same time, the decomposition mode of the complexed β-CD is greatly changed. This investigation would contribute to a better understanding of the intermolecular interactions in host−guest chemistry and further to the application of the solid inclusion complexes of β-CD in medicine, food additives, biological products, and so on.

Acknowledgment. We thank the NSFC (No. 29601005) for financial support. We would like to acknowledge the assistance of H. Yin in the GC-TOF-MS measurements of this investigation and in useful discussions.

References and Notes

(1) Liu, Y.; Cao, R.; Chen, Y.; He, J. Y. *J. Phys. Chem. B* **2008**, *112*, 1445–1450.
(2) Muller, A.; Wenz, G. *Chem. Eur. J.* **2007**, *13*, 2218–2223.
(3) Zhu, X. L.; Wang, H. B.; Chen, Q.; Yang, W. C.; Yang, G. F. *J. Agric. Food Chem.* **2007**, *55*, 3535–3539.
(4) Hădărugă, N. G.; Hădărugă, D. I.; Păunescu, V.; Tatu, C.; Ordodi, V. L.; Bandur, G.; Lupea, A. X. *Food Chem.* **2006**, *99*, 500–508.
(5) Scalia, S.; Tursilli, R.; Sala, N.; Iannuccelli, V. *Int. J. Pharm.* **2006**, *320*, 79–85.
(6) Denadai, A. M. L.; Teixeira, K. I.; Santoro, M. M.; Pimenta, A. M. C.; Cortes, M. E.; Sinisterra, R. D. *Carbohydr. Res.* **2007**, *342*, 2286–2296.
(7) Ma, M. G.; Zhu, Y. J. *Mater. Lett.* **2008**, *62*, 2512–2515.
(8) Hsu, Y. J.; Lu, S. Y.; Lin, Y. F. *Chem. Mater.* **2008**, *20*, 2854–2856.
(9) Khan, S.; Nami, S. A. A.; Siddiqi, K. S. *Spectrochim. Acta, Part A* **2007**, *68*, 269–274.
(10) Yoshii, H.; Neoh, T. L.; Beak, S. H.; Furuta, T. *J. Inclusion Phenom. Macrocyclic Chem.* **2006**, *56*, 113–116.
(11) Yuan, C.; Jin, Z. Y.; Xu, X. M.; Zhuang, H. N.; Shen, W. Y. *Food Chem.* **2008**, *109*, 264–268.
(12) Lahiani-Skiba, M.; Coquard, A.; Bounoure, F.; Verite, P.; Arnaud, P.; Skiba, M. *J. Inclusion Phenom. Macrocyclic Chem.* **2007**, *57*, 197–201.
(13) Aki, H.; Niiya, T.; lwase, Y.; Kawasaki, Y.; Kumai, K.; Kimura, T. *Thermochim. Acta* **2004**, *416*, 87–92.
(14) Song, L. X.; Teng, C. F.; Xu, P.; Wang, H. M.; Zhang, Z. Q.; Liu, Q. Q. *J. Inclusion Phenom. Macrocyclic Chem.* **2008**, *60*, 223–233.
(15) Song, L. X.; Teng, C. F.; Wang, H. M.; Bai, L. *Chin. J. Chem. Phys.* **2008**, *21*, 174–180.
(16) Liu, L.; Guo, Q. X. J. *J. Inclusion Phenom. Macrocyclic Chem.* **2002**, *42*, 1–14.
(17) Garcia-Zubiri, I. X; Gonzalez-Gaitano, G.; Isasi, J. R. *Thermochim. Acta* **2006**, *444*, 57–64.
(18) Reija, B.; Al-Soufi, W.; Novo, M.; Tato, J. V. *J. Phys. Chem. B* **2005**, *109*, 1364–1370.
(19) Wang, H. M.; Song, L. X.; Teng, C. F.; Bai, L. *Chin. J. Inorg. Chem.* **2008**, *24*, 1–9.
(20) Gabelica, V.; Galic, N.; De Pauw, E. *J. Am. Soc. Mass Spectrom.* **2002**, *13*, 946–953.
(21) Arakawa, R.; Yamaguchi, T.; Takahashi, A. *J. Am. Soc. Mass Spectrom.* **2003**, *14*, 1116–1122.
(22) Yu, Z.; Cui, M.; Yan, C. Y.; Song, F. R.; Liu, Z. Q.; Liu, S. Y. *Rapid Commun. Mass Spectrom.* **2007**, *21*, 683–690.
(23) Wei, M.; Wang, J.; He, J.; Evans, D. G.; Duan, X. *Microporous Mesoporous Mater.* **2005**, *78*, 53–61.
(24) Banerjee, S. S.; Chen, D. *Chem. Mater.* **2007**, *19*, 6345–6349.
(25) Xu, P.; Song, L. X.; Wang, H. M. *Thermochim. Acta* **2008**, *469*, 36–42.
(26) Éhen, Zs.; Giordano, F.; Sztatisz, J.; Jicsinszky, L.; Novák, Cs. *J. Therm. Anal. Calorim.* **2005**, *80*, 419–424.
(27) Fernandes, L. P.; Éhen, Zs.; Moura, T. F.; Novák, Cs.; Sztatisz, J. *J. Therm. Anal. Calorim.* **2004**, *78*, 557–573.
(28) Song, L. X.; Wang, H. M.; Xu, P.; Zhang, Z. Q.; Liu, Q. Q. *Bull. Chem. Soc. Jpn.* **2007**, *80*, 2313–2322.

JP806026Q